

Correlation of Morphology and Function of Flecks Using Short-Wave Fundus Autofluorescence and Microperimetry in Patients With Stargardt Disease

Patty P. A. Dhooge^{1,*}, Esmee H. Runhart^{1,*}, Stanley Lambertus¹, Nathalie M. Bax¹, Johannes M. M. Groenewoud², B. Jeroen Klevering¹, and Carel B. Hoyng¹

¹ Department of Ophthalmology, Radboud University Medical Center, Nijmegen, The Netherlands

² Department for Health Evidence, Radboud University Medical Center, Nijmegen, The Netherlands

Correspondence: Carel B. Hoyng, Department of Ophthalmology, Radboud University Medical Center, P.O. Box 9101, 6500 HB Nijmegen, The Netherlands.
e-mail: carel.hoyng@radboudumc.nl

Received: September 7, 2020

Accepted: December 7, 2020

Published: March 18, 2021

Keywords: stargardt disease (STGD); ATP-binding cassette transporter A4 (ABCA4); microperimetry; short-wavelength autofluorescence (SW-AF) imaging; autofluorescence

Citation: Dhooge PPA, Runhart EH, Lambertus S, Bax NM, Groenewoud JMM, Klevering BJ, Hoyng CB. Correlation of morphology and function of flecks using short-wave fundus autofluorescence and microperimetry in patients with stargardt disease. *Trans Vis Sci Tech.* 2021;10(3):18, <https://doi.org/10.1167/tvst.10.3.18>

Purpose: The purpose of this study was to evaluate the functional relevance of longitudinal changes in hyperautofluorescent areas and flecks in Stargardt disease (STGD1) using short-wavelength autofluorescence (SW-AF) imaging.

Methods: In this prospective, longitudinal study, 31 patients with STGD1 (56 eyes) underwent microperimetry (MP) and SW-AF imaging twice in 3 to 5 years. A total of 760 MP test points were included in the statistical analysis based on stable fixation and accurate alignment of SW-AF and MP. Autofluorescence intensity was qualitatively assessed in all MP test points. Small circumscriptive hyperautofluorescent lesions were defined as flecks. Longitudinal imaging characteristics observed on SW-AF were classified into the following categories: appearing, disappearing, and stable flecks, stable hyperautofluorescent, and stable background autofluorescence. The relationship between SW-AF intensity changes and MP changes was analyzed using a linear mixed model corrected for baseline sensitivity.

Results: Retinal sensitivity declined most in locations without change in SW-AF intensity. Functional decline per year was significantly larger in flecks that disappeared (-0.72 ± 1.30 dB) compared to flecks that appeared (-0.34 ± 0.65 dB), if baseline sensitivity was high (≥ 10 dB; $P < 0.01$). The correlation between the change observed on SW-AF and the sensitivity change significantly depended on the sensitivity at baseline ($P = 0.000$).

Conclusions: Qualitative longitudinal assessment of SW-AF poorly reflected the retinal sensitivity loss observed over the course of 3 to 5 years.

Translational Relevance: When aiming to assess treatment effect on lesion level, a multimodal end point including MP focused on hyperautofluorescent lesions appears essential but needs further studies on optimizing MP grids, eye-tracking systems, and alignment software.

Introduction

Autosomal recessive Stargardt disease (STGD1) is the most prevalent inherited macular dystrophy and there currently are no viable treatment options.¹ In STGD1, mutations in the gene encoding the ATP-binding cassette transporter A4 (ABCA4) impair the removal of retinal from the photoreceptor disks and retinal pigment epithelium (RPE) endolysosomes,

which results in lipofuscin accumulation in the RPE.^{2,3} Over time, this leads to destruction of both the RPE and the overlying photoreceptors with severe visual impairment as a result.⁴⁻⁶ In recent years, different treatment options for STGD1 have been in development, some of which are currently being tested in clinical trials. Strategies vary from stem-cell therapy and genetic therapy (e.g. gene augmentation therapy with lentiviruses; and RNA therapy with antisense oligonucleotides) to pharmacological agents aimed

at preventing lipofuscin accumulation.^{7,8} However, because STGD1 has a relative slow rate of progression and sensitive end points, to test the benefit of these newly found therapies have not been established yet.

Yellow-white flecks and chorioretinal atrophy centered around the posterior pole are the hallmark features of STGD1. These lesions can be readily distinguished on ophthalmoscopy, although these are better delineated using short-wavelength fundus autofluorescence (SW-AF) imaging. SW-AF imaging typically shows intensely fluorescent pisciform flecks in the macula, often extending to the midperiphery, and macular hypo-autofluorescent areas corresponding to areas of RPE atrophy.^{9–11} SW-AF imaging allows for objective and fast measurement of the extent of RPE atrophy, which has been correlated to loss of function measured using microperimetry (MP) and visual acuity.^{12–14} Therefore, RPE atrophy measured using SW-AF imaging has become a major biomarker of disease progression and an end point in three out of six phase II/III clinical trials for STGD1 (Supplementary Table S1). However, RPE atrophy growth generally is slow and variable, both challenging the ability of this biomarker to detect short-term treatment effect.^{15–18} Additionally, the potential of this imaging biomarker as a primary end point is limited by trial design (e.g. trials in early disease stages, prior to RPE atrophy).

The potential of hyperautofluorescence and particularly flecks, an early hallmark of STGD1, as a biomarker for progression is less evident. The small, pisciform lesions that appear hyperautofluorescent on SW-AF imaging correspond to hyper-reflective bands on spectral-domain optical coherence tomography.¹⁹ In longitudinal natural history studies, flecks centrifugally expand outward from the central macula and their intensity on SW-AF imaging increases and subsequently declines over time leaving residual atrophy.^{20–26} Especially these regions of visible disease activity in early stages might be interesting loci to include in a progression biomarker. Previous studies also demonstrated a characteristic general background increase in autofluorescence signal in patients with STGD1.²⁷ In clinical trials, especially those aimed at lipofuscin reduction, these autofluorescence patterns might serve as a biomarker to prove treatment effect. Knowledge on the correlation between autofluorescence patterns and retinal function is required to assess the potential of SW-AF imaging change as treatment outcome, because primary efficacy end points in late-phase clinical trials should reflect clinical benefit to provide substantial evidence of effectiveness.²⁸

MP is a fundus guided visual field test, which enables functional follow-up of selected retinal areas or lesions

in time. Microperimetric mean sensitivity showed a decline within 1 year in patients with STGD1 and may therefore serve as a useful end point for clinical trials.^{29,30} Indeed, STGD1 flecks that appear hyperautofluorescent on SW-AF imaging have been associated with a significantly lower retinal sensitivity, measured by MP, compared to the nearest non-flecked areas. Conversely the sensitivity of these hyperautofluorescent flecks is significantly higher compared to hypoautofluorescent flecks.^{31,32} On the other hand, nasal and temporal segments of STGD1 eyes with elevated levels of autofluorescence had preserved retinal sensitivity.³³ However, longitudinal data on the correlation between autofluorescence patterns of lipofuscin-laden regions on SW-AF imaging during follow-up and retinal function still are limited. The purpose of this study is to correlate SW-AF imaging changes, especially in hyperautofluorescent flecks and areas with retinal sensitivity change measured using MP.

Methods

Subjects

This prospective, longitudinal study was conducted at the Department of Ophthalmology at the Radboud University Medical Center. This study was approved by the local ethics committee and adhered to the tenets of the Declaration of Helsinki. All patients gave written informed consent prior to enrollment.

Patients with a clinical diagnosis of STGD1, supported by the identification of one or two disease-causing *ABCA4* alleles were included between 2013 and 2015. The clinical diagnosis was made based on the presence of macular, irregular shaped flecks, that appear yellow-white on ophthalmoscopy, hyperautofluorescent on SW-AF imaging in combination with progressive macular atrophy. Participants underwent MP and SW-AF imaging during 2 visits; visit 1 between 2013 and 2015 and visit 2 in 2018. Other variables collected were best-corrected visual acuity (Snellen), age at onset, and disease duration. Age at onset was defined as the onset of first visual complaints attributable to STGD1 disease reported by the patient. The disease duration was defined as the time between the age at onset and the study visit.

Image Acquisition and Selection of Eyes

Macular sensitivity was assessed by performing MP with the Nidek MP1 (Nidek Technologies, Padova, Italy). This system ensures the correct projection of stimuli on the corresponding infrared (IR)

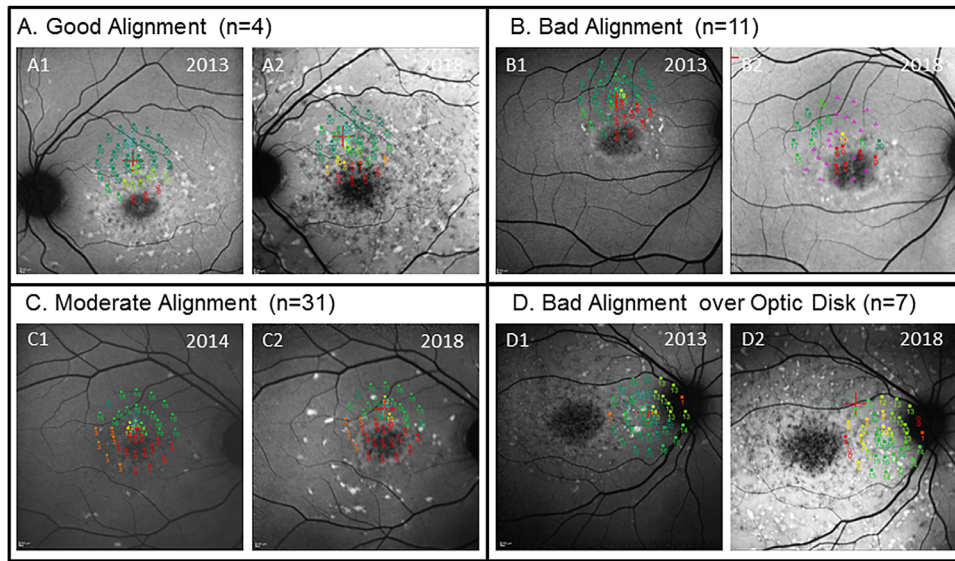


Figure 1. Examples of quality assessment of the data alignment between both visits, after coregistration of MP with SW-AF images. The data of the first visit (images A1, B1, C1, and D1) was compared to data of the second visit (images A2, B2, C2, and D2).

ophthalmoscopic image of the retina by using an integrated eye tracking system. Each MP measurement was performed under mesopic light conditions and prior to SW-AF imaging. The nontested eye was occluded. Patients were asked to focus on a 2 degrees diameter red fixation target, leading to the preferred retinal loci (PRL) as the center of the MP grid. Full-threshold fundus perimetry was performed by using a 4-2-1 staircase and 40-point strategy. Goldmann II standard size stimuli were presented for 200 milliseconds. Eight points were tested at 1 degree from the PRL, and 16 points were tested at 3 degrees and 5 degrees from the PRL, respectively. The Nidek MP1 simultaneously assesses fixation stability based on the Fujii criteria.³⁴ Fixation was classified as “stable” when 75% of fixations were located within a 2 degrees diameter circle; as “relatively unstable” if $\geq 75\%$ of fixations were located within a 4 degrees diameter circle and as “unstable” if $< 75\%$ of fixations were located within a 4 degrees diameter circle. An MP training program was performed prior to the baseline test to reduce learning effects. During follow-up, the manufacturer’s follow-up protocol was used.

SW-AF images were taken using a confocal scanning laser ophthalmoscope with an optically pumped solid-state laser with 488-nm excitation (Spectralis; Heidelberg Engineering, Heidelberg, Germany) after adequate pupil dilatation. En face SW-AF images of 30 degrees and 55 degrees were acquired (Automatic Real Time [ART] ≥ 15).

Using the Microperimeter MP1 software (Navis Software, version 1.7; Nidek Technologies, Inc.)

SW-AF images were imported and coregistered with the MP data. Two retinal vessel bifurcations in each image were selected as coregistration landmarks. To correct for distortion, the quality of the alignment was judged by two independent graders (P.P.A.D. and E.H.R.). Alignment of MP1 with SW-AF imaging between baseline and follow-up was compared and qualitatively classified as “good” (MP test points on the exact same location), “moderate” (MP test points partially overlapped), or “bad” (MP test points did not overlap or macular sensitivity > 0 was measured in the optic disk; Fig. 1).

Eyes were excluded from further analyses if the image quality was poor ($n = 3$), alignment of the multimodal imaging was considered bad ($n = 18$), or the fixation was unstable at either visit ($n = 33$). As a result, only 19 eyes of 12 patients fitted both the fixation and alignment criteria and were included in the analysis. Supplementary Figure S1 and Supplementary Table S2 gives a detailed overview of the selected eyes.

Image Grading

The SW-AF imaging intensity relative to the image background was graded at each point of the MP grid. Hence, points were qualified as background autofluorescence, hyperautofluorescent (more intense than background), or hypo-autofluorescent (less intense than background; Fig. 2). Hyperautofluorescent lesions were further divided into hyperautofluorescent areas (characteristic pattern of diffuse background increase of SW-AF imaging)³⁵ or an STGD1 fleck

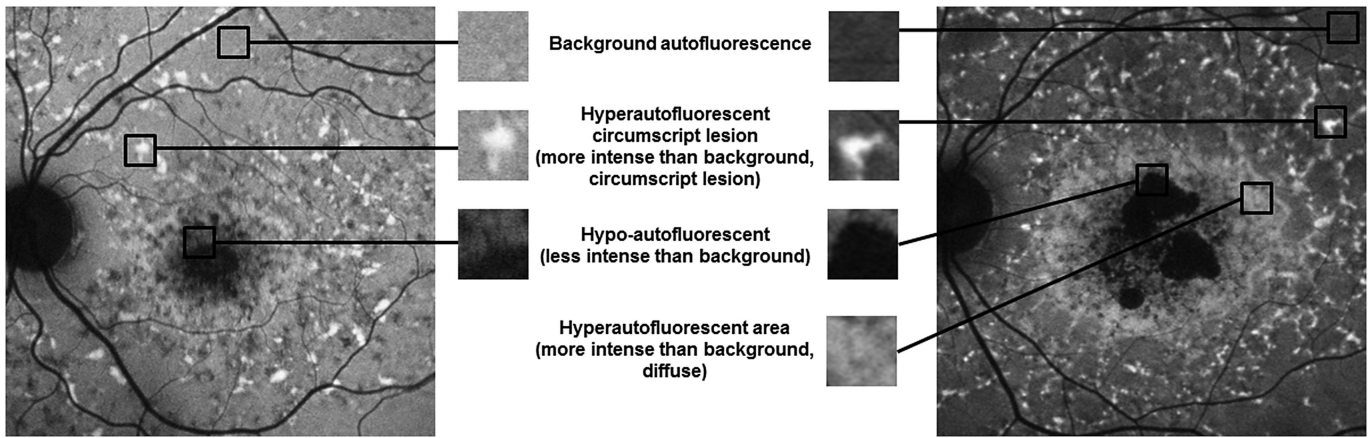


Figure 2. At the MP test points SW-AF imaging intensity was graded as background autofluorescence, hyperautofluorescent area, hyperautofluorescent circumscriptive lesion (fleck), or hypo-autofluorescent.

Table. Categories of Longitudinal SW-AF Characteristics

Category	SW-AF Visit 1	SW-AF Visit 2
Stable background autofluorescence (<i>n</i> = 303)	Background autofluorescence	Background autofluorescence
Stable hyperautofluorescent (<i>n</i> = 17)	Hyperautofluorescent area	Hyperautofluorescent area
Stable fleck (<i>n</i> = 17)	Hyperautofluorescent circumscript lesion	Hyperautofluorescent circumscript lesion
Appearing fleck (<i>n</i> = 26)	Background autofluorescence	Hyperautofluorescent circumscript lesion
Disappearing fleck, change to hypo-autofluorescent (<i>n</i> = 26)	Hyperautofluorescent circumscript lesion	Hypo-autofluorescent
Disappearing fleck, change to hyperautofluorescent (<i>n</i> = 12)	Hyperautofluorescent circumscript lesion	Hyperautofluorescent area

SW-AF, short-wavelength fundus autofluorescence imaging.

(small hyperautofluorescent circumscriptive lesion).¹⁹ Grading was performed by two independent graders (P.P.A.D. and E.H.R.) and was discussed until agreement was reached.

Based on the cross-sectional SW-AF imaging grading, five categories of longitudinal SW-AF imaging characteristics were defined, as specified in the [Table](#).

Statistical Analysis

The correlation between image characteristics and microperimetry was assessed using a linear mixed model, in which the functional change in MP over time was the dependent variable and the SW-AF imaging category was the main independent variable. We accounted for variations between patients and between the eyes of each patient by using two levels. All measurements were nested within the eyes (eyes as level) and the eyes were nested within the patients (patients as level). To correct for possible confounding, the following continuous covariables were considered: baseline macular sensitivity, follow-up time, and disease duration. From the possible confounders, only baseline sensitivity appeared to be associated with functional change. In order to provide a better insight

in the relationship between the functional change and the two predictors, we also modeled baseline microperimetry as a dichotomous instead of a continuous outcome variable. For this purpose, macular sensitivity 0 to 9 was labeled as “low MP,” and macular sensitivity 10 to 20 was labeled as “high MP.” A *P* < 0.05 was considered to be statistically significant.

Results

Thirty-one patients with STGD1 (10 men and 21 women) were enrolled in this study. Four patients had early-onset STGD1 (age at onset ≤ 10 years), 22 patients had intermediate-onset STGD1 (age at onset 11–44 years), and 5 patients had late-onset STGD1 (age at onset ≥ 45 years). Median follow-up time was 4 years (range = 3–5 years). At follow-up, the mean age was 45 ± 15 years (range = 20–69 years), and the mean visual acuity in the right eye and left eye was 20/143 (decimal = 0.14 ± 0.22 , range = 0.16–0.80) and 20/200 (decimal = 0.10 ± 0.14 , range = 0.02–1.0), respectively. None of the patients had concomitant ocular disease and all included eyes were phakic with clear media. The participants’ characteristics are described in Supplementary Table S3.

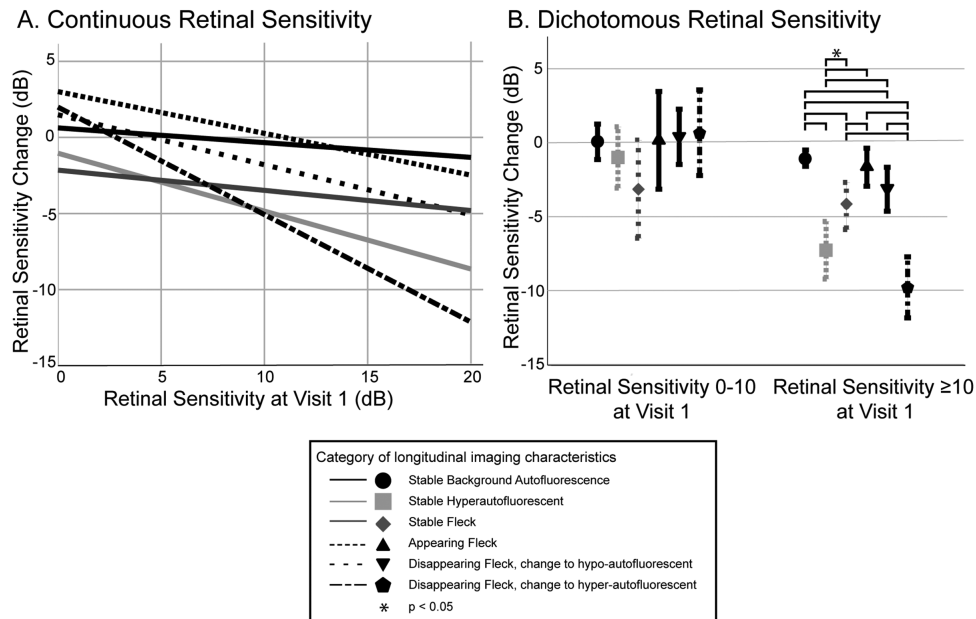


Figure 3. The linear mixed model shows that the retinal sensitivity change over time not only depends on the longitudinal SW-AF imaging intensity over time but also on the baseline sensitivity as is depicted in (A). Although no SW-AF imaging change over time was observed in lesions of category “stable hyperautofluorescent,” the retinal sensitivity in these loci decreased. (B) Displays the model-estimated marginal means and 95% confidence interval per defined category. Significant differences in functional decline were found between several categories in regions with high initial sensitivity. * $P < 0.05$.

Because of fixation and alignment criteria only 19 of 56 eyes were included in the analysis. A total of 760 MP test points (40 locations for each eye) were categorized based on the corresponding local autofluorescence intensity. Two hundred sixty-four locations were graded as hyperautofluorescent, of which 98 MP test points were located on a fleck. Mean retinal sensitivity in these flecks was 11.75 ± 6.88 dB. Between baseline and follow-up, 38 of these flecks disappeared and 26 flecks appeared. Mean baseline sensitivity of appearing flecks (16.69 ± 5.24 dB) was higher compared to disappearing flecks (10.32 ± 7.75 dB) and the estimated functional decline per year was larger (-0.34 ± 0.65 dB in appearing flecks and -0.72 ± 1.30 dB in disappearing flecks). Retinal sensitivity did not change over time when background SW-AF imaging intensity remained constant (i.e. the category “stable background autofluorescence” [-0.16 ± 0.51 dB per year]).

A linear mixed model was conducted to model the sensitivity change as a function of the longitudinal imaging characteristics, the baseline sensitivity, and the interaction term of the latter two. The other covariables “follow-up time” and “disease duration” had no significant correlation with the sensitivity change over time and were therefore not used in the model.

The effect of the longitudinal SW-AF imaging category on the sensitivity change over time signifi-

cantly depended on the baseline sensitivity (interaction baseline sensitivity * SW-AF imaging change, $P = 0.000$): as expected, the retinal sensitivity showed a larger decline if the sensitivity at baseline was relatively preserved. The relation between the retinal sensitivity and the defined categories of longitudinal imaging characteristics is visualized in Figure 3. Regions of hyperautofluorescence at baseline showed the largest sensitivity decline. Interestingly, the retinal sensitivity declined most in regions that did not show a change in SW-AF imaging intensity over time (i.e. regions that remained hyperautofluorescent). The model with retinal sensitivity as a dichotomous variable (see Fig. 3B) clearly shows significant differences in functional decline between the several defined categories in regions with high initial sensitivity.

Discussion

This study addressed the relationship between qualitatively assessed longitudinal imaging characteristics on SW-AF imaging and retinal sensitivity over time. Knowledge on the correlation between autofluorescence patterns and retinal function is required to assess these biomarkers as treatment outcome, because primary efficacy end points in late-phase clinical trials

should reflect clinical benefit to provide substantial evidence of effectiveness. To allow for adequate assessment of SW-AF imaging changes and the retinal sensitivity in time on lesion level, we included 19 out of 56 eyes (34%), of 12 out of 31 patients, because the other eyes had a bad fixation or there was an improper alignment of the examination modalities of follow-up to baseline. For the longitudinal analysis of subfield sensitivity variables in ProgStar Report No. 13, the use of follow-up function and good or fair pattern placement limited the count of eyes from 359 to 106 (30%).²⁹ Limitations that cause this loss of data mostly relate to inclusion of patients with advanced disease stage. Despite the use of the integrated eye-tracking system, unstable fixation impaired the reliability of MP measurements. Additionally, the coregistration of MP and SW-AF imaging may have been imperfect because manual coregistration using two landmarks does not correct for distortion. We have corrected this by strictly assessing the quality of the alignment. However, inadequate alignment could have affected the accuracy of the correlation between SW-AF imaging and MP to some degree. In order to obtain comparable MP measurements over time, we used the same hardware and software between 2013 and 2018. However, techniques used in microperimetry have been improved. Next to this, recent advances in imaging techniques have provided new ways to assess the characteristics of flecks (e.g. fluorescence lifetime imaging ophthalmoscopy and quantitative autofluorescence).^{36,37} With these techniques, longitudinal imaging characteristics can be assessed in a quantitative way instead of via qualitative analysis as we did in this study. In order to longitudinally study the retinal sensitivity in specific lesions in more detail, new data should be obtained using the most recent advancements in technology. Despite the limitations we encountered, a total of 760 MP test points were considered as well aligned and of sufficient quality to accurately assess the correlation between the longitudinal SW-AF imaging characteristics and the retinal sensitivity.

Mean retinal sensitivity in flecks was comparable to the 12.89 ± 3.86 dB reported by others.³¹ This study also supports the evidence that background autofluorescence, which is generally hyperautofluorescent in STGD1 eyes as compared with normal eyes, is not associated with loss of function.^{27,33} To our best knowledge, there are no previous reports on the correlation between autofluorescence patterns during follow-up and retinal function. Our data demonstrated that the retinal sensitivity declined in loci where a new fleck appeared as well as in loci where a fleck disappeared, during a follow-up time of 3 to 5 years. Moreover, loci of stable flecks and disappearing flecks

showed a larger functional decrease than loci of flecks that arose. These data fit the hypothesis that, during the pathological process of flecks appearing, fading, and leaving residual atrophy, the retinal sensitivity shows a progressive decline over time, and progression rate might even increase during this process.⁴⁻⁶

The structural basis of flecks is still under debate. Because lipofuscin accumulation in RPE cells is one of the hallmarks in STGD pathogenesis, flecks have long been assumed to be lipofuscin-laded RPE cells.^{2,3,38} Recent examination of flecks across multiple imaging modalities indicated that flecks might reflect groups of photoreceptor cells degenerating after the loss of RPE.³⁷ Yet, recent histology correlations suggest that flecks corresponded to subretinal macrophages packed with pigment granules (lipofuscin, melanin, and melanolipofuscin).³⁹ Our data show that retinal sensitivity in flecks is not lost and even can remain stable during several years of follow-up. Therefore, our data contradict hypotheses of flecks representing dead photoreceptor cells. Further work is required to establish the histopathological substrate of flecks.

In the hyperautofluorescent regions and flecks that did not show SW-AF imaging change over time, the retinal sensitivity declined most according to the statistical model. Because of the inability to distinguish qualitative differences, SW-AF imaging does not seem a good measure of preservation of function. The same was concluded from the observation that areas of reduced AF were not compatible with the area of dense scotoma in patients with STGD1.⁴⁰ In our post hoc analysis, the functional decline in a stable fleck was significantly larger compared to stable background autofluorescence regions and appearing flecks, when sensitivity at baseline was defined as high (>10 dB). Because these histopathological changes over time were not discernable with SW-AF imaging only, a multimodal end point approach is needed when it comes to selecting outcome measures for clinical trials.

This study focused on hyperautofluorescent lesions as the autofluorescent pattern of lipofuscin might serve as a biomarker to prove treatment effect of clinical trials aiming at lipofuscin reduction. When the tested loci were hyperautofluorescent at baseline (i.e. the defined categories stable hyperautofluorescent, stable fleck, and disappearing fleck), they showed a larger decline in sensitivity as compared to loci that were hypo-autofluorescent or the same level as the background autofluorescence at baseline. This makes baseline hyperautofluorescence an interesting biomarker as it might predict a functional decline over time in those areas. Baseline retinal sensitivity might serve as inclusion criterium for clinical trials, despite the described limitations of MP, because our data showed

that regions with higher sensitivity at baseline allowed for a better differentiation of sensitivity changes over time in relation to SW-AF imaging changes over time.

In conclusion, SW-AF imaging does not adequately reflect the retina's functional change over time and, therefore, is not suitable as the sole primary end point in trials. For the evaluation of hyperautofluorescence and STGD1 flecks in clinical trials, a multimodal end point including MP focused on hyperautofluorescent lesions could have great potential. However, further studies that make use of improved eye-tracking systems as well as advanced software to allow accurate coregistration of retinal examination modalities are required to assess the added value of MP in a multimodal end point.

Acknowledgments

Supported by Stichting AF Deutman oogheelkunde researchfonds Nijmegen (Grant to B.J.K. and C.B.H.) and the Foundation Fighting Blindness USA, Grant No. PPA-0517-0717-RAD (Grant to F.P.M.C., S.R., and C.B.H.).

Disclosure: **P.P.A. Dhooge**, None; **E.H. Runhart**, None; **S. Lambertus**, None; **N.M. Bax**, None; **J.M.M. Groenewoud**, None; **B.J. Klevering**, None; **C.B. Hoyng**, None

* PPAD and EHR contributed equally to this work and share first authorship.

References

- Birtel J, Eisenberger T, Gliem M, et al. Clinical and genetic characteristics of 251 consecutive patients with macular and cone/cone-rod dystrophy. *Sci Rep*. 2018;8:4824.
- Allikmets R, Singh N, Sun H, et al. A photoreceptor cell-specific ATP-binding transporter gene (ABCR) is mutated in recessive Stargardt macular dystrophy. *Nat Genet*. 1997;15:236–246.
- Lenis TL, Hu J, Ng SY, et al. Expression of ABCA4 in the retinal pigment epithelium and its implications for Stargardt macular degeneration. *Proc Natl Acad Sci U S A*. 2018;115:E11120–E11127.
- Sparrow JR, Gregory-Roberts E, Yamamoto K, et al. The bisretinoids of retinal pigment epithelium. *Prog Retin Eye Res*. 2012;31:121–135.
- Weng J, Mata NL, Azarian SM, Tzekov RT, Birch DG, Travis GH. Insights into the function of Rim protein in photoreceptors and etiology of Stargardt's disease from the phenotype in abcr knock-out mice. *Cell*. 1999;98:13–23.
- Cideciyan AV, Aleman TS, Swider M, et al. Mutations in ABCA4 result in accumulation of lipofuscin before slowing of the retinoid cycle: a reappraisal of the human disease sequence. *Hum Mol Genet*. 2004;13:525–534.
- Sears AE, Bernstein PS, Cideciyan AV, et al. Towards treatment of Stargardt disease: workshop organized and sponsored by the Foundation Fighting Blindness. *Transl Vis Sci Technol*. 2017;6:6.
- Lu LJ, Liu J, Adelman RA. Novel therapeutics for Stargardt disease. *Graefes Arch Clin Exp Ophthalmol*. 2017;255:1057–1062.
- Kellner S, Kellner U, Weber BH, Fiebig B, Weinitz S, Ruether K. Lipofuscin- and melanin-related fundus autofluorescence in patients with ABCA4-associated retinal dystrophies. *Am J Ophthalmol*. 2009;147:895–902, 902.e891.
- Charbel Issa P, Barnard AR, Singh MS, et al. Fundus autofluorescence in the Abca4(-/-) mouse model of Stargardt disease—correlation with accumulation of A2E, retinal function, and histology. *Invest Ophthalmol Vis Sci*. 2013;54:5602–5612.
- Kuehlewein L, Hariri AH, Ho A, et al. Comparison of manual and semiautomated fundus autofluorescence analysis of macular atrophy in Stargardt disease phenotype. *Retina*. 2016;36:1216–1221.
- Cideciyan AV, Swider M, Aleman TS, et al. Macular function in macular degenerations: repeatability of microperimetry as a potential outcome measure for ABCA4-associated retinopathy trials. *Invest Ophthalmol Vis Sci*. 2012;53:841–852.
- Parodi MB, Iacono P, Triolo G, et al. Morphofunctional correlation of fundus autofluorescence in Stargardt disease. *Br J Ophthalmol*. 2015;99:1354–1359.
- Schonbach EM, Wolfson Y, Strauss RW, et al. Macular sensitivity measured with microperimetry in Stargardt disease in the progression of atrophy secondary to Stargardt Disease (ProgStar) study: report no. 7. *JAMA Ophthalmol*. 2017;135:696–703.
- Chen B, Tosha C, Gorin MB, Nusinowitz S. Analysis of autofluorescent retinal images and measurement of atrophic lesion growth in Stargardt disease. *Exp Eye Res*. 2010;91:143–152.
- Fujinami K, Lois N, Mukherjee R, et al. A longitudinal study of Stargardt disease: quantitative assessment of fundus autofluorescence, progression, and genotype correlations. *Invest Ophthalmol Vis Sci*. 2013;54:8181–8190.

17. McBain VA, Townend J, Lois N. Progression of retinal pigment epithelial atrophy in Stargardt disease. *Am J Ophthalmol.* 2012;154:146–154.
18. Strauss RW, Kong X, Ho A, et al. Progression of Stargardt disease as determined by fundus autofluorescence over a 12-month period: ProgStar Report No. 11. *JAMA Ophthalmol.* 2019;137(10):1134–1145.
19. Sparrow JR, Marsiglia M, Allikmets R, et al. Flecks in recessive Stargardt disease: short-wavelength autofluorescence, near-infrared autofluorescence, and optical coherence tomography. *Invest Ophthalmol Vis Sci.* 2015;56:5029–5039.
20. Cukras CA, Wong WT, Caruso R, Cunningham D, Zein W, Sieving PA. Centrifugal expansion of fundus autofluorescence patterns in Stargardt disease over time. *Arch Ophthalmol.* 2012;130:171–179.
21. Gomes NL, Greenstein VC, Carlson JN, et al. A comparison of fundus autofluorescence and retinal structure in patients with Stargardt disease. *Invest Ophthalmol Vis Sci.* 2009;50:3953–3959.
22. Lois N, Halfyard AS, Bird AC, Holder GE, Fitzke FW. Fundus autofluorescence in Stargardt macular dystrophy-fundus flavimaculatus. *Am J Ophthalmol.* 2004;138:55–63.
23. Smith RT, Gomes NL, Barile G, Busuioc M, Lee N, Laine A. Lipofuscin and autofluorescence metrics in progressive STGD. *Invest Ophthalmol Vis Sci.* 2009;50:3907–3914.
24. Fishman GA, Stone EM, Grover S, Derlacki DJ, Haines HL, Hockey RR. Variation of clinical expression in patients with Stargardt dystrophy and sequence variations in the ABCR gene. *Arch Ophthalmol.* 1999;117:504–510.
25. Armstrong JD, Meyer D, Xu S, Elfervig JL. Long-term follow-up of Stargardt's disease and fundus flavimaculatus. *Ophthalmology.* 1998;105:448–457; discussion 457–448.
26. Chen L, Lee W, de Carvalho JRL, et al. Multiplatform imaging in ABCA4-associated disease. *Sci Rep.* 2019;9:6436.
27. Burke TR, Duncker T, Woods RL, et al. Quantitative fundus autofluorescence in recessive Stargardt disease. *Invest Ophthalmol Vis Sci.* 2014;55:2841–2852.
28. US Department of Health & Human Services, US Food and Drug Administration. Human Gene Therapy for Retinal Disorders: Guidance for Industry. Available at: <https://www.hhs.gov/guidance/document/human-gene-therapy-retinal-disorders-guidance-industry>.
29. Schönbach EM, Strauss RW, Muñoz B, et al. Longitudinal microperimetric changes of macular sensitivity in Stargardt disease after 12 months: ProgStar Report No. 13. *JAMA Ophthalmol.* 2020;138:772–779.
30. Testa F, Melillo P, Di Iorio V, et al. Macular function and morphologic features in juvenile Stargardt disease: longitudinal study. *Ophthalmology.* 2014;121:2399–2405.
31. Verdina T, Tsang SH, Greenstein VC, et al. Functional analysis of retinal flecks in Stargardt disease. *J Clin Exp Ophthalmol.* 2012;3:10.4172/2155-9570.1000233.
32. Muller PL, Birtel J, Herrmann P, Holz FG, Charbel Issa P, Gliem M. Functional relevance and structural correlates of near infrared and short wavelength fundus autofluorescence imaging in ABCA4-related retinopathy. *Transl Vis Sci Technol.* 2019;8:46.
33. Müller PL, Gliem M, McGuinness M, Birtel J, Holz FG, Charbel Issa P. Quantitative fundus autofluorescence in ABCA4-related retinopathy - functional relevance and genotype-phenotype correlation. *Am J Ophthalmol.* 2021;222:340–350.
34. Fujii GY, de Juan E, Sunness J, Humayun MS, Pieramici DJ, Chang TS. Patient selection for macular translocation surgery using the scanning laser ophthalmoscope. *Ophthalmology.* 2002;109:1737–1744.
35. Kumar V. Insights into autofluorescence patterns in Stargardt macular dystrophy using ultra-wide-field imaging. *Graefes Arch Clin Exp Ophthalmol.* 2017;255:1917–1922.
36. Solberg Y, Dysli C, Escher P, Berger L, Wolf S, Zinkernagel MS. Retinal flecks in Stargardt disease reveal characteristic fluorescence lifetime transition over time. *Retina.* 2019;39:879–888.
37. Paaavo M, Lee W, Allikmets R, Tsang S, Sparrow JR. Photoreceptor cells as a source of fundus autofluorescence in recessive Stargardt disease. *J Neurosci Res.* 2019;97:98–106.
38. Eagle RC, Lucier AC, Bernardino VB, Yanoff M. Retinal pigment epithelial abnormalities in fundus flavimaculatus: a light and electron microscopic study. *Ophthalmology.* 1980;87:1189–1200.
39. Fang Y, Tschulakow A, Taubitz T, et al. Fundus autofluorescence, spectral-domain optical coherence tomography, and histology correlations in a Stargardt disease mouse model. *FASEB J.* 2020;34:3693–3714.
40. Sunness JS, Steiner JN. Retinal function and loss of autofluorescence in Stargardt disease. *Retina.* 2008;28:794–800.